STUDY ON THE SURFACE MORPHOLOGY AND FRACTAL CHARACTERISTICS OF GRANITE UNDER THERMAL SHOCK OF SEAWATER

by

Hu-Chao DENG[a], Jian-Jun HU[b*], Gui-Kang LIU[a*], Si-Qi YE[a], and Da-Li SUN[c]

[a]College of Water Resource and Hydropower, Sichuan University, Chengdu, China
[b]Guangdong Provincial Key Laboratory of Deep Earth Sciences and Geothermal Energy Exploitation and Utilization, Shenzhen University, Shenzhen, China
[c]Jinshi Drilltech Co. Ltd., Tangshan, China

Original scientific paper
https://doi.org/10.2298/TSCI2301571D

Geothermal energy has become one of the new energy sources of great concern due to its wide distribution, abundant reserves and green, clean and renewable advantages. In view of the advantages of both geothermal energy development potential and abundant seawater reserves in the coastal areas, granite is taken as the research object, and the surface topography under different temperatures (100 °C, 200 °C, 300 °C, 400 °C, and 500 °C) and different thermal shock cycles (0, 5, 10, 15 and 20) is obtained. Based on 3-D scanning technology, the damage details of the surface are reconstructed, and the roughness parameters of the surface are obtained. The maximum height, the maximum valley depth and the arithmetic mean height increase with the increase of the temperature and the number of times, but the maximum peak height does not change significantly. Based on fractal theory, the variation law of the fractal dimension is further discussed. The impact regions that affect the fractal dimension and thermal damage are divided: the weak impact region, the transition region, and the significant impact region. It lays a corresponding basic law for the heat exchange efficiency and strength characteristics of dry hot rock.

Key words*: energy evolution, dry hot rock, seawater thermal shock, surface morphology, fractal theory*

Introduction

The energy problem in the global perspective is prominent, and the environmental problem is significant. The massive development and consumption of traditional fossil energy is an important reason for the high carbon emissions. Therefore, marching into the deep part of the earth [1, 2] and seeking new green energy from the source has become an important solution. Under the background of gradual exploration of deep underground resources [3-6], geothermal energy has been paid much attention and expected in the field of new energy due to its wide distribution, abundant reserves and green, clean and renewable advantages [7, 8]. The enhanced geothermal systems (EGS) [9] proposed by Los Alamos National Laboratory

*Corresponding authors, e-mail: hujianjun@cumt.edu.cn; liuguikang1996@outlook.com

(LANL) in America is mainly used for the geothermal development of deep dry hot rock. In the process of EGS geothermal reservoir construction, the physical and mechanical response of dry hot rock under the impact of cold and hot cycles does not be ignored. Scholars have carried out basic research on the physical and mechanical response of dry hot rock under thermal shock [10]. After thermal shock, the physical and mechanical properties of granite deteriorate to a certain extent, including longitudinal wave velocity [11, 12], elastic modulus and compressive strength [13, 14]. With the increase of thermal shock cycle times, granite will gradually induce more microcracks [13], and the appearance of more cracks leads to the increase of permeability [15]. Different types of cold and thermal cycle treatments also have different effects on physical and mechanical parameters [16-18], and rapid quenching has more significant effects on granite samples [15, 19]. The granite temperature has a significant effect on its mechanical properties [20]. Different temperature gradients are set and mechanical tests are conducted. The rock stress-strain curve model [21] and the particle mechanics model [22] are also established. It is concluded that the thermal induced microcracks are the main factors leading to the degradation of rock mechanical properties [23-25]. The research shows that the granite generally tends to decrease with the increase of granite occurrence temperature and the increase of cold and thermal cycles, and its physical and mechanical properties deteriorate to a certain extent, which is mainly due to the thermal damage of granite under thermal shock [26]. Therefore, the thermal damage of granite after thermal shock has also been studied [27]. The thermal damage is mainly caused by the expansion of mineral particles and the formation of cracks, and the critical temperature that ultimately leads to rock damage is 250 ℃ [28]. The mechanical properties, porosity and permeability of rocks change significantly with thermal expansion and structural damage [29, 30].

Most of the existing studies focus on the physical and mechanical properties of granite from a macro perspective, but little attention is paid to the area with the most significant thermal impact. Therefore, in this study, granite is taken as the research object, the research on the surface morphology of granite under different temperatures and different cold and thermal shock times are systematically carried out. Then the evolution characteristics of surface morphology characteristics is described with impact temperature and times by various parameters characterizing the surface roughness, and the damage degree of granite surface is quantitatively characterized by fractal theory. Thus, it lays a foundation for the study of thermal conductivity and mechanical properties of granite.

Sample preparation and test plan

Sample preparation

The same complete rock mass was selected in the sample preparation process, and the drilling was consistent, and the surface was free of macroscopic cracks. The granite is processed to a diameter of 50 mm and length of 100 mm recommended by ISRM. The average density is 2.617 g/cm^3. The seawater used to cool the high-temperature granite is manually configured, tab. 1. The density of the solution is 1.05-1.06 g/cm^3 and the pH value is 8.2.

Table 1. Composition table of prepared seawater

Component	Content [gL^{-1}]	Component	Content [gL^{-1}]	Component	Content [gL^{-1}]
NaCl	26.518	$MgSO_4$	3.305	$MgCl_2$	2.447
$CaCl_2$	1.141	KCl	0.725	$NaHCO_3$	0.202
NaBr	0.083	–	–	–	–

Test scheme and test instrument

The specific process is as follows, fig. 1:

– The prepared samples are put into CR-MJ5 muffle furnace, the sample to the design temperature (100 °C, 200 °C, 300 °C, 400 °C, and 500 °C, respectively) are heated at a heating rate of 5 °C per minutes and keep it for 4 hours, and then the high temperature granite is placed immediately in a cooling tank filled with seawater in room temperature.
– After the sample is cooled to room temperature, it is taken out and dried in DHG-9035 drying oven for 24 hours to conduct the next high-temperature thermal shock test.
– Repeat 1st and 2nd steps, and conduct natural cooling (0 times) for the samples at five design temperatures in turn, and rapid cooling in seawater for 5 times, 10 times, 15 times, and 20 times.
– The surface topography data of the sample under various conditions are obtained through VR-5000-3D Profile, and further research on the surface topography and fractal characteristics is carried out.

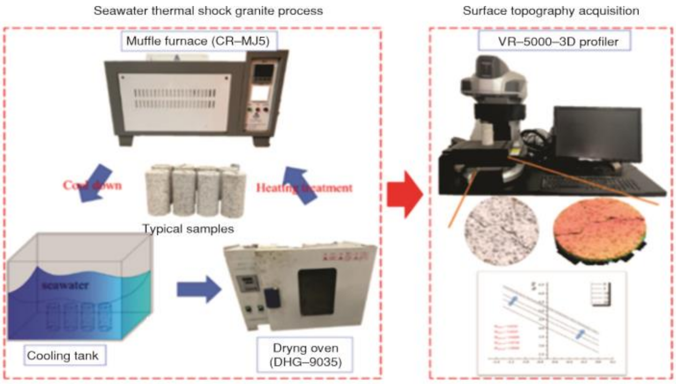

Figure 1. Experimental instruments and test procedures

Results

Surface morphology of granite after thermal shock

Under the shock of seawater at room temperature, the surface of high temperature granite cools rapidly. Due to the rapid circulation of cold and heat for many times, the granite has different height and depth features on the surface, and even obvious macro cracks appear. In order to describe the morphological characteristics of granite surface, the contour scanner VR-5000-3D is used to accurately measure the height fluctuation of the surface. The typical scanning results (200 °C and 500 °C) are shown in fig. 2. The results indicate that the surface of high temperature granite is impacted by seawater and its morphological characteristics have changed significantly. Therefore, the change of its unevenness will be quantitatively characterized by some characteristic parameters.

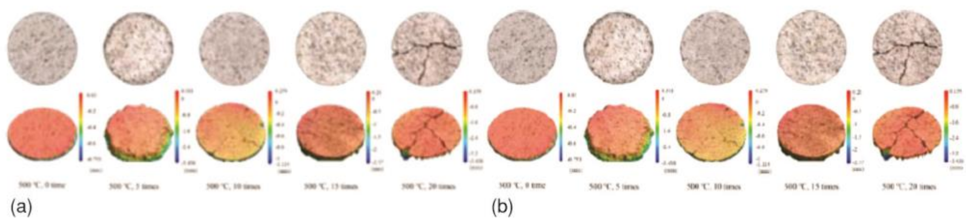

Figure 2. Surface morphology of granite under the impact of seawater cold and hot cycles; (a) under 200 °C and (b) under 500 °C

Surface roughness of granite after thermal shock

The international roughness test standard ISO 25178 is adopted, in which four important surface topography parameters are defined, namely, the maximum peak height, *Sp*, the maximum Valley depth, *Sv*, the maximum height, *Sz*, and the arithmetic average height, *Sa*.

In the ISO 25178, *Sp* represents the highest height of the peak on the granite surface, and *Sv* represents the lowest height of the valley on the surface. The *Sv* represents the height difference between the highest peak vertex and the lowest valley bottom point, so the three satisfy the relationship as shown in eq. (1). The data point model obtained by the contour scanner to obtain *Sp*, *Sv*, and *Sz* is analyzed, as shown in figs. 3 and 4. There is the relation:

$$Sz = Sp + Sv \tag{1}$$

where *Sz* is the maximum height, *Sp* – maximum peak height, and *Sv* – maximum valley depth.

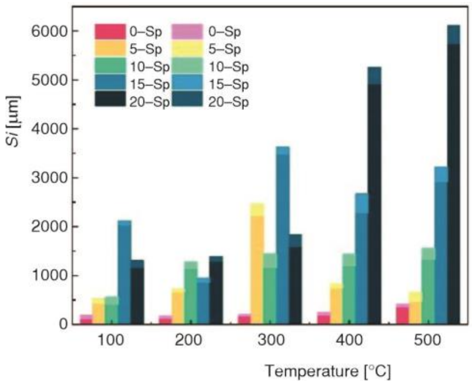

Figure 3. Relationship between roughness parameters and temperature

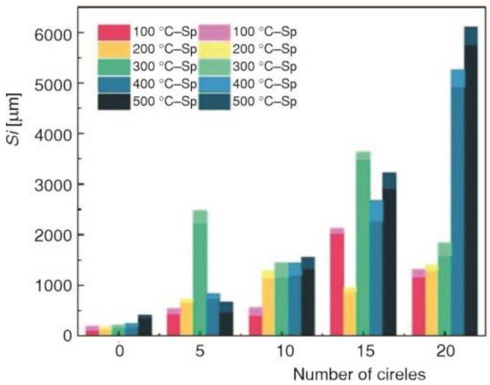

Figure 4. Relationship between roughness parameters and the number of cycles

The stacking histogram is formed by superimposing *Sv* in the lower half and *Sp* in the upper half. The superimposed histogram shows the maximum height of the granite surface. From the relationship between the roughness parameters and the granite temperature and the number of cold and thermal cycles, it can be seen that when the cold and thermal shock cycle is not carried out, *Sv* is close to *Sp* at the beginning, which is about 100 μm. With the increase of the number of cycles, the values of *Sv* showed an obvious upward trend. After the number of cold and hot cycles are 15, the depth increases sharply. After 20 cold and hot cycles at 500 ℃, the depth was 16 times that of the initial state. On the contrary, *Sp* did not change significantly, and its value remained at 100-300 μm, which is not as obvious as the value of *Sv*. With the increase of granite surface temperature, the values of *Sv* and *Sp* show a similar law to the number of cycles, that is, *Sv* gradually increases while *Sp* has no obvious change. It is worth noting that when the temperature reaches 300 ℃ or above, the rising trend of *Sv* is further intensified. Under the strong influence of *Sv* and the weak influence of *Sp*, *Sz* of the granite surface is basically consistent with *Sv*.

The arithmetic mean height *Sa*, that is, the average value of the average plane height difference, is one of the most widely used parameters. It is not significantly affected by scratches, contamination, and measurement noise. Therefore, figs. 5 and 6 are obtained. At a certain temperature of granite, the average height of its surface always shows a gradual growth trend. When the temperature is 100 ℃ and 200 ℃, *Sa* increases slowly, the average growth rate of *Sa* is 30.85% at 200 ℃, and when the temperature rises to 300 ℃ and above, *Sa* increases rapidly. The average growth rate can reach 148.69% at 500 °C, which indicates that the surface roughness is limited when the temperature is low (< 300 °C) while the temperature becoming higher (≥ 300 °C), the surface roughness changes significantly. Except for 0 time, the *Sa* of the granite surface shows a trend of gradually increasing. When the cold and thermal cycles reach 15 times or more, the surface roughness *Sa* increases further. This indicates that only high- temperature treatment of granite will not change the surface roughness. The thermal impact of its high temperature surface and seawater is the fundamental reason for the change of surface roughness.

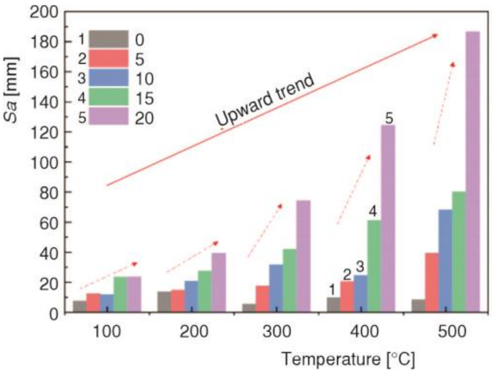

Figure 5. Relationship between arithmetic mean height *Sa* and temperature

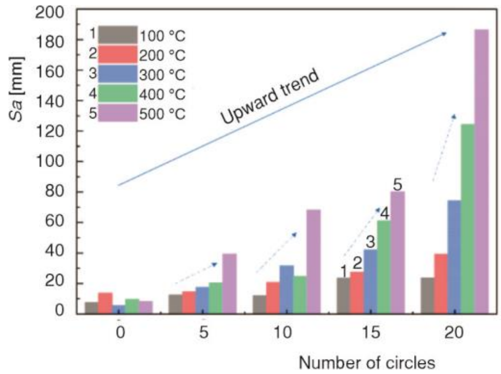

Figure 6. Relationship between arithmetic mean height *Sa* and the number of cycles

Discussion

In order to characterize this change, the traditional roughness expression method does not quantitatively characterize the degree of rise and fall of granite surface as a whole. Fractal geometry theory is an important new method to analyze the rock surface topography and fracture distribution in geotechnical engineering [31]. Fractal dimension is the most important index to measure the complexity and irregularity of fractal volume in fractal theory, and also an important parameter to reflect the degree of fractal self-similarity [32, 33]. Therefore, cube covering method is adopted for fractal theory analysis. In this method, the granite surface is covered by a cube with side length a, and the total number of cubes $N(a)$ required to cover the joint surface is calculated. The total number of cubes $N(a)$ measured at different scales a is plotted on the double logarithmic coordinate map. The slope of the straight line $N(a)$ is given by:

$$N(a) \sim a^{-D} \tag{2}$$

which implies that

$$D = -\frac{\lg N(a)}{\lg a} \tag{3}$$

where D is the fractal dimension and a is the side length of a cube. It has been reported (2) was considered to model the elasticity [34] and flows [35, 36].

The fractal dimensions of each sample surface are obtained, and the fractal dimensions are shown in fig. 7. The surface temperature of granite has a significant influence on the surface morphology of granite. The average fractal dimension at each temperature is 2.03471, 2.04737, 2.06900, 2.07371, and 2.07763, respectively, which indicates that the average fractal dimension of granite surface increases gradually with the increase of temperature. It is consistent with the results of traditional roughness characterization. On the other hand, with the increase of the number of cycles, the fractal dimension of the sample surface mainly shows an upward trend. Different from the law of roughness characterization, when the number of cycles is 0, the fractal dimension still gradually increases with the temperature. In the case of low cycle times, a large range of slight thermal damage will occur on the granite surface, and the difference between the high and low fluctuations is small. The reason why the average height change is not obvious in *Sa* is that *Sa* can only be considered from the height, but cannot characterize the large range of thermal damage on the surface. The fractal dimension can better characterize the influence degree of thermal damage due to the self-similar property.

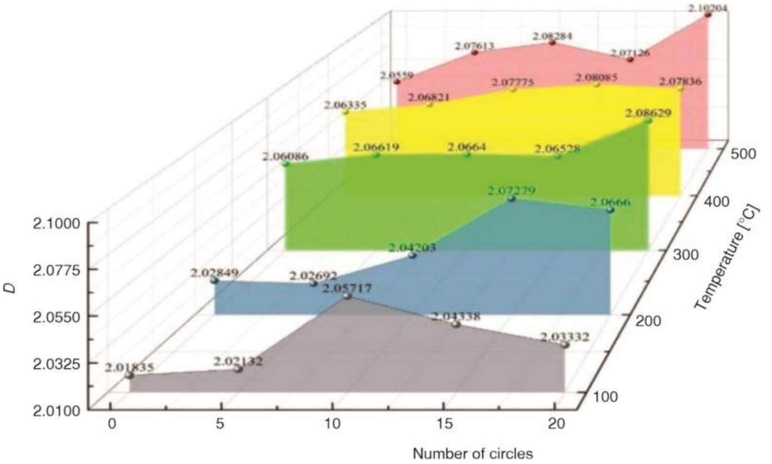

Figure 7. Relationship among fractal dimension, temperature and cycle times of granite surface

The 3-D fitting of the relationship among the fractal dimension, temperature and the number of cycles is carried out under thermal damage. The results show that the fitting is good, of which correlation coefficient reaches 0.92, fig. 8. In general, the conditions of lower temperature and lower number of cold and thermal cycles have less influence on the fractal dimension of granite surface, while the conditions of higher temperature and higher number of cycles have greater influence on the fractal dimension of granite surface. Based on the degree of the influence, the impact region can be divided for the top view of the fitting image. The region in the blue wireframe in fig. 8 is divided into the weak impact region, which is mainly in the low cycle number region with low temperature. The fractal dimension of this area is maintained at 2.02~2.04, and is weakly affected by thermal damage; The area in the yellow wireframe is defined as the transition region, which is mainly under the working conditions of 10 and 15 cycles of low temperature and 5 and 10 cycles of high temperature. The fractal dimension is kept at 2.05~2.06, and the surface roughness changes obviously. It is subject to a certain degree of thermal shock, which results in slight erosion. The area in the red wireframe is defined as a significant impact region, which is mainly concentrated in the working conditions of relatively low temperature and high cycle times. Under the working conditions of relatively high temperature and high cycle times, the fractal dimension is distributed between 2.07 and 2.10, and the surface topography characteristics change significantly. Under the repeated thermal shock of high temperature granite and seawater, the granite surface and its internal temperature gradient change, and the uneven expansion of minerals causes the change of granite morphology characteristics. The surface erosion is serious, and even obvious macro cracks are formed. With the increase of temperature and cycle times, the surface thermal damage is more serious, which is reflected in the increase of roughness and fractal dimension.

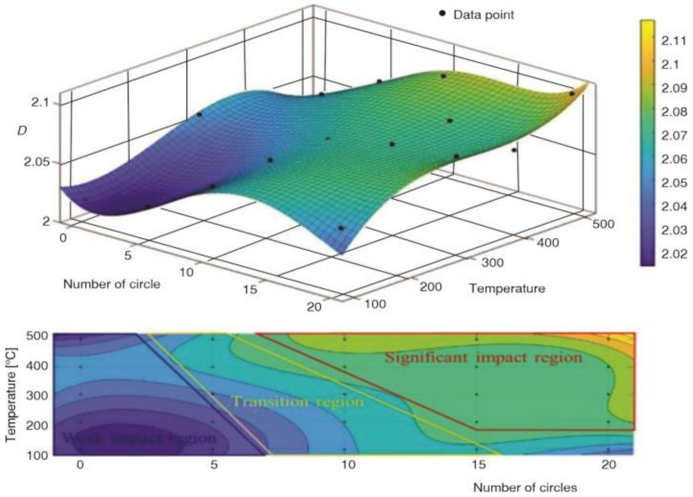

Figure 8. Fitting of fractal dimension *D*, temperature and cycle number of granite surface

Conclusion

In the study, the surface morphology of granite has changed obviously after multiple thermal shock with seawater under high temperature. After thermal shock of high temperature granite and seawater, *Sv* of surface roughness parameter gradually increases with the increase of temperature and cycle times, while *Sp* does not change significantly, and *Sz* gradually increases under the strong influence of *Sv*. The growth of *Sz* and *Sv* was further intensified after the temperature was 300 ℃ and the number of cycles was 15. This indicates that the seawater thermal shock produces erosion and damage to the surface. The mean height *Sa* of granite surface after seawater thermal shock can more stably represent the degree of thermal damage. Under lower temperature conditions (100 ℃ and 200 ℃), *Sa* increases slowly. When the temperature continues to rise, *Sa* increases rapidly. If the number of cycles are given as 15, the values of *Sa* are increasing rapidly. This indicates that the surface roughness is limited when the temperature is lower (< 300 ℃), and the surface roughness changes significantly when the temperature is higher (≥ 300 ℃). With the increase of temperature and the number of cycles, the fractal dimensions gradually increase, which is basically consistent with the rule of roughness. Three impact region affecting the fractal dimension of granite surface are divided: the weak impact region (D = 2.02~2.04) is distributed in the area of low temperature and low cycle times, and the surface is slightly damaged by heat; The transition region (D = 2.05~2.06) is distributed in the low temperature (10~15 cycles) and high temperature (5~10 cycles) regions, causing certain thermal damage and denudation; The significant impact region (D = 2.07~2.10) is distributed in the area with high temperature and high cycle number, and the thermal damage is serious and even macro cracks appear.

Acknowledgment

This work was financially supported by the Shenzhen Basic Research (General Project) (JCYJ20190808153416970), the Shenzhen National Science Fund for Distinguished

Young Scholars (RCJC20210706091948015), and the China Postdoctoral Science Foundation (2022M722178).

Nomenclature

Sp	– maximum peak height, [μm]	*Sa*	– arithmetic average height, [μm]
Sv	– maximum valley depth, [μm]	*N*	– number of cubes, [–]
Sz	– maximum height, [μm]	*D*	– the fractal dimensions [–]

References

[1] Gao, M. Z., *et al*., In-Situ Disturbed Mechanical Behavior of Deep Coal Rock, *Journal of China Coal Society, 45* (2020), 8, pp. 2691-2703
[2] Gao, M. Z., *et al*., Progress in Research on Deep in Situ Rock Mechanics, *Bulletin of National Natural Science Foundation of China, 35* (2021), 6, pp. 895-903
[3] Gao, M. Z., *et al*., Mechanical Behavior of Coal under Different Mining Rates: A Case Study From Laboratory Experiments To Field Testing, *International Journal of Mining Science Technology, 31* (2021), 5, pp. 825-841
[4] Gao, M. Z., *et al*., Calculating Changes in Fractal Dimension of Surface Cracks to Quantify How the Dynamic Loading Rate Affects Rock Failure in Deep Mining, *Journal of Central South University, 27* (2020), 10, pp. 3013-3024
[5] Gao, M. Z., *et al*., Discing Behavior and Mechanism of Cores Extracted from Songke-2 Well at Depths below 4500 m, *International Journal of Rock Mechanics and Mining Sciences, 149* (2022), 104976
[6] Gao, M. Z., *et al*., The Mechanism of Microwave Rock Breaking and Its Potential Application to Rock-Breaking Technology in Drilling, *Petroleum Science, 19* (2022), 3, pp. 1110-1124
[7] Xie, H. P., *et al*., Assessment of Geothermal Resource Potential in the Guangdong-Hong Kong-Macao Greater Bay Area, *Journal of Sichuan University, 51* (2019), 1, pp. 1-8
[8] Zhang, J. Q., *et al*., Improvement Research of Condensing Equipment in Organic Rankine Cycle Power Generation Systems, *Thermal Science, 25* (2021), 1B, pp. 491-501
[9] Norbeck, J. H., *et al*., Analysis of Hydromechanical Reservoir Response during Fluid Circulation at the Fenton Hill Enhanced Geothermal System Test Site, *Proceedings*, 44th New Zealand Geothermal Workshop, Auckland, New Zealand, 2016
[10] Wang, X. Z., *et al*., Mechanical Properties and Acoustic Emission Characteristics of Granite under Thermo-Hydro-Mechanical Coupling, *Thermal science, 25* (2021), 6B, pp. 4585-4596
[11] Zhang, Y., *et al*., Pore, Mechanics and Acoustic Emission Characteristics of Limestone under the Influence of Temperature, *Applied Thermal Engineering*, *123* (2017), Aug., pp. 1237-1244
[12] Wu, Z. S., *et al*., Study on Law of Longitudinal Wave Velocity Evolution of Dry Hot Rock after Thermal Shock, *Coal Science and Technology*, *49* (2021), 10, pp. 58-65
[13] Yu, P., *et al*., Physico-Mechanical Properties of Granite after Cyclic Thermal Shock, *Journal of Rock Mechanics and Geotechnical Engineering*, *12* (2020), 4, pp. 693-706
[14] Zhang, H. W., *et al*., High Temperature Mechanical Properties and Thermal Shock Effect of Hot Dry Rock, *Journal of Mining and Safety Engineering*, *38* (2021), 1, pp. 138-145
[15] Jin, P., *et al*., Influence of Different Thermal Cycling Treatments on the Physical, Mechanical and Transport Properties of Granite, *Geothermics*, *78* (2019), Mar., pp. 118-128
[16] Xi, B. P., *et al*., Experimental Investigations of Compressive Strength and Thermal Damage Capacity Characterization of Granite under Different Cooling Modes, *Chinese Journal of Rock Mechanics and Engineering*, *39* (2020), 2, pp. 286-300
[17] Xi, B. P., *et al*., Evolution of Mechanical Properties of Granite under Thermal Shock in Water with Different Cooling Temperatures, *Rock and Soil Mechanics*, *41* (2020), S1, pp. 83-94
[18] Xi, B. P., *et al*., Experimental Study on the Relationship between Macroscopic Mechanical Parameters of Granite and Thermal Shock Velocity under Thermal Shock, *Chinese Journal of Rock Mechanics and Engineering*, *38* (2019), 11, pp. 2194-2207
[19] Hu, J. J., *et al*., Changes in the Thermodynamic Properties of Alkaline Granite after Cyclic Quenching Following High Temperature Action, *International Journal of Mining Science and Technology*, *31* (2021), 5, pp. 843-852
[20] Kumari, W. G. P., *et al*., Temperature-Dependent Mechanical Behaviour of Australian Strathbogie Granite with Different Cooling Treatments, *Engineering Geology*, *229* (2017), 7, pp. 31-44

[21] Peng, J., *et al*., Physical and Mechanical Behaviors of a Thermal-Damaged Coarse Marble under Uniaxial Compression, *Engineering Geology*, *200* (2016), 18, pp. 88-93
[22] Zhao, Z. H., *et al*., Shear Behavior of Beishan Granite Fractures after Thermal Treatment, *Engineering Fracture Mechanics*, *213* (2019), 15, pp. 223-240
[23] Hu, J, *et al*., Variation of Mechanical Properties of Granite after High-Temperature Treatment, *Arabian Journal of Geosciences*, *11* (2018), 2, 43
[24] Sun, Q, *et al*., The Effect of Rapid Cooling on the Thermal Diffusivity of Granite, *Journal of Applied Geophysics*, *168* (2019), Sept., pp. 71-78
[25] Sun, Q., *et al*., Effects of Heating on Some Physical Properties of Granite, Shandong, China, *Journal of Applied Geophysics, 193* (2021), 104410
[26] Shen, Y., *et al*., Thermal Deterioration of High-Temperature Granite after Cooling Shock: Multiple-Identification and Damage Mechanism, *Bulletin of Engineering Geology and the Environment*, *79* (2020), 10, pp. 5385-5398
[27] Wang, H., *et al*., Coupling Characteristics of Meso-Structure and Thermophysical Parameters of Deep Granite under High Geo-Temperature, *Thermal science*, *25* (2021), 6B, pp. 4621-4629
[28] Dong, Z., *et al*., Thermal Damage of Granite after Thermal Shock Cycle, *Geotechnique Letters*, *10* (2020), 1, pp. 1-6
[29] Inserra, C., *et al*., Influence of Thermal Damage on Linear and Nonlinear Acoustic Properties of Granite, *International Journal of Rock Mechanics and Mining Sciences*, *62* (2013), Sept., pp. 96-104
[30] Kompanikova, Z., *et al*., Sandstone Alterations Triggered by Fire-Related Temperatures, *Environmental Earth Sciences*, *72* (2014), Mar., pp. 2569-2581
[31] Xie, H. P., *et al*., Fractal Fracture and Fragmentation in Rocks, *Journal of Disaster Prevention and Mitigation Engineering*, *23* (2003), 4, pp. 1-9
[32] Xie, J., *et al*., Experimental Investigation on Anisotropic Fractal Characteristics of The Rock Fracture Surface and Its Application on the Fluid Flow Description, *Journal of Petroleum Science and Engineering*, *191* (2020), 107190
[33] Gao, M. Z., *et al*., Fractal Evolution and Connectivity Characteristics of Mining-Induced Crack Networks in Coal Masses at Different Depths, *Geomechanics and Geophysics for Geo-Energy and Geo-Resources*, *7* (2021), 1, 9
[34] Yang, X. J., *et al.*, On the Theory of the Fractal Scaling-law Elasticity, *Meccanica*, *57* (2022), 4, pp. 943-955
[35] Yang, X. J., An Insight on the Fractal Power Law Flow: from a Hausdorff Vector Calculus Perspective, *Fractals*, *30* (2022), 3, pp. 2250054-929
[36] Yang, X. J., The Vector Power-Law Calculus with Applications in Power-Law Fluid Flow, *Thermal Science*, *24* (2020), 6B, pp. 4289-4302

Paper submitted: August 27, 2022
Paper revised: November 13, 2022
Paper accepted: November 24, 2022